Process windows for shell hardening of unalloyed steel cylinders due to high speed quenching

T. Lübben, F. Frerichs

Kobasko et. al. have shown that rapid water quenching can create compressive residual stresses near the surface and hereby a significant increase of the fatigue-limit results (Intensive Quenching). Depending on steel grade, dimensions of the component and quenching intensity through hardening or only shell hardening will result. In this work shell hardening processes were investigated in a more detailed manner for cylinders made out of two different unalloyed steels. The goal of the work was the finding of general requirements to reach on one hand a sufficient surface hardness paired with a non through hardened hardening profile. On the other hand compressive residual stresses in the near surface area should be produced as high as possible to receive huge live time cycles of the heat treated work pieces. To reach this aim quenching experiments with cylinders made out of SAE 1035 (C35) and SAE 1055 (C56E2) were done by use of a special facility for high speed quenching (heat transfer coefficients (HTC) up to ≈100.000 W/m²K). Parallel this process was modelled by a Finite Element approach which was validated by comparison with experimentally achieved data. By use of this model the process windows were determined. They provide the heat treating expert the opportunity to estimate HTC values as a function of cylinder radius which fulfil the conditions for shell hardening and compressive residual stresses at the surface.

KEYWORDS: HIGH SPEED QUENCHING - SHELL HARDENING - COMPRESSIVE RESIDUAL STRESSES - UNALLOYED STEEL - PROCESS WINDOW - HEAT TREATMENT SIMULATION

INTRODUCTION

The benefits of Intensive Quenching (IQ) are well known, a relevant summary can be found in [1]. In this paper the focus will be on single piece High-Speed Quenching (HSQ). The difference between this process and the corresponding IQ process is the missing interrupt of the intensive cooling at the time when the compressive surface stresses are at their maximum value.

Former investigations showed that if shafts of a given material were through hardened, the residual stress state depends only on the Biot number [2, 3]. This dimensionless number is here defined by:

$$Bi = \frac{\alpha}{\lambda_m} \cdot \frac{V}{S} \qquad (1)$$

α: mean heat transfer coefficient of the process	[W/(m²K)]
λ: mean heat conductivity of the shaft material	[W/(mK)]
V, S: volume and surface of the shaft	[m³], [m²]

It was shown that a critical Biot number for compressive residual stresses at the surface exists. If the applied Biot number of a given process is larger than the critical one, compressive residual stresses at the surface occur. In this regard it is irrelevant at which values of heat transfer coefficient, heat conductivity, and volume to surface ratio the Biot number is calculated. Only the actual result is relevant [2, 3].

During a through hardening process only the temperature depending martensitic transformation must be considered. Therefore the critical Biot number depends mainly on the two parameters of the Koistinen Marburger law for martensite formation [4]. But what happens with the stress development during quenching if the process does not result in a through

Thomas Lübben, Friedhelm Frerichs
Stiftung Institut für Werkstofftechnik (IWT), Bremen, Germany

Paper presented at European Conference on Heat Treatments ECHT 2015 and 22nd IFHTSE Congress, Venice 20-22 May 2015 - organised by AIM

hardened state? In this case time dependent transformation processes occur. The additionally formed phase bainite and possibly ferrite and pearlite have furthermore lower densities and different mechanical properties than martensite. From these facts it can be concluded that the Biot number solely is not sufficient for the characterization of the residual stress state. At least an explicit dependence on the radius of the shaft should result. Consequently the process windows depend on steel grade, geometry, and dimensions.

In this paper the procedure for the detection of the process windows for shafts made of two unalloyed steels will be presented. The investigations were focused on shell hardening. Therefore the first goal was finding a suitable distribution of microstructure and hardness respectively. The second aim was the development of high compressive residual stresses in the surface near area of the work piece.

The experimental conditions of this work will be described in section 1. The achievable heat transfer coefficients (HTC) with the equipment of IWT Bremen will be characterized in section 2. Hardness and residual stress measurements will be presented in section 3. Finally the process windows and their dependence on carbon content will be shown in section 4.

EXPERIMENTAL CONDITIONS

Steel grades and samples

In order to investigate steel grades with significantly different phase transformation kinetics the unalloyed carbon steel C35 (SAE 1035) and the unalloyed bearing steel C56E2 (SAE 1055) were chosen. Table 1 shows the chemical composition of the two steel grades. Fig. 1 shows CCT-diagrams based on dilatometer tests. SAE 1055 has in comparison to SAE 1035 a lower martensite start temperature (M_s) and a smaller critical cooling rate for martensite formation. Furthermore its martensite has a larger specific volume and a higher hardness after quenching. More details about the determination of the CCT diagrams and the other simulation relevant parameters are given in [5, 6].

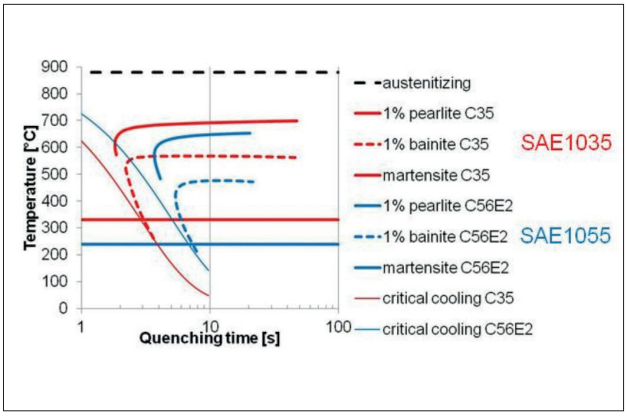

Fig. 1 - CCT diagrams based on measurements for the simulation studies

Tab. 1 - Chemical composition of investigated steels (mass %)

	C	Si	Mn	Ni	Cr	Mo	V
SAE 1035	0,34	0,24	0,72	0,08	0,21	0,02	0,003
SAE 1055	0,56	0,283	0,822	0,092	0,174	0,0265	0,003

The investigated shafts were cylindrical with a constant length of 150 mm. The variations of the shaft radius are given in Table 2.

Tab. 2 - Investigated values of shaft radius

	Radius (mm)			
SAE 1035	12,5	15	17,5	20
SAE 1055		15	18,3	21,7

Heat treatment

The shafts were austenitized for 30 min in a tube furnace with nitrogen atmosphere at 880 °C. Afterwards the shafts were automatically lowered into the subjacent quenching tool (for more details see [2, 3]). Two different types of tools were used. The first type produces an annular gap flow (Fig. 2, left). In this case the quenching medium flows from top to bottom through a gap that is formed by the inner tube of the tool and the quenched shaft inside. The gap width is constant over the complete tool and is defined by the difference of inner tube radius and shaft radius. The medium velocity in the gap is given by the quotient of pump rate and gap cross sectional area. The pump capacity is in the range of 8 to 16 l/s which leads to mean medium velocities up to 10 m/s. After starting the quenching process it takes about 0.3 s until the steady state flow is formed. Because of the cap for flow guidance (Fig. 2) the water flow settles down, which leads to a less turbulent media flow. For this tool type two different inner tube radii were applied, 60 and 90 mm.

In the second type of quenching tool the outer gap is closed at the top (Fig. 2, right). The connection between outer and inner gap consists of 12 rows each with 8 nozzles in circumferential direction and a diameter of 4 mm. The mean flow velocity in the plane of a nozzle exit is in the range of 6.6 - 13.3 m/s. The conical shape of this tool and the increasing gap width lead to a homogenization of the resulting HTC distribution. Nevertheless, the HTC distribution depends strongly on position, because

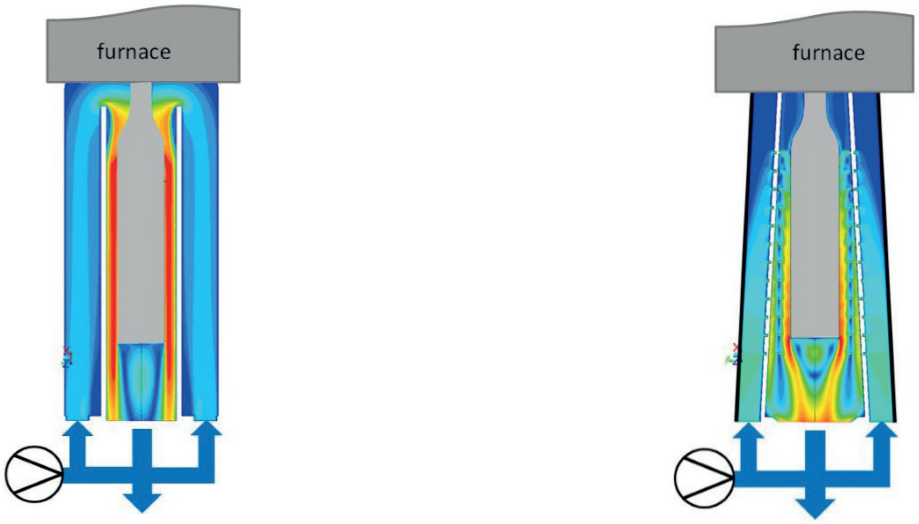

Fig. 2 - Schematic drawings of quenching tools at IWT with flow field distributions of water velocity: left: gap flow right: jets

directly below a jet the HTC is higher than between the jets. But inside the shafts the huge heat conductivity of steel smoothes the cooling inhomogeneities very effective, which leads to quite homogeneous microstructure and residual stresses. In all experiments tap water or a 10% salt-water-solution respectively with temperatures of 20 to 25°C were used. Tempering processes were not executed.

ACHIEVABLE HEAT TRANSFER COEFFICIENTS

Temperature measurements were performed with a copper cylinder (Ø 40 mm) quenched in the above described quenching tools. The copper cylinder was equipped with thermocouples placed near the surface in the mid plane of the cylinder. To avoid boiling processes its initial temperature was approximately 100°C. For more experimental details see [7].

Fig. 3 presents measured HTC values which were produced with a quenching tool with gap flow and an inner diameter of 60mm. At the beginning of the process the heat transfer coefficient increases and reaches the end value after about 0.2 to 0.4 s. The figure includes furthermore a comparison of these measurements with calculated data by use of empirical equations for a gap flow [8]. The agreement between measurement and calculation is excellent. Hence the empirical equations can be used for the calculation of the HTC for other shaft and inner tube radii.

Fig. 4 summarizes the HTC determinations for different medium velocities and quenching tools. Principally the tools generate increasing HTC with increasing flow velocity. But a small influence of the inner tube radius can be seen, too. The jet quenching tool produces much higher HTC values (approximately by a factor two). The figure includes a comparison of the measurements with results of Computational Fluid Dynamic simulations, too. Again the agreement is quite well. Only for higher water velocities an underestimation can be observed. Nevertheless, simulation by CFD can predict the HTC for jet quenching in an acceptable quality, which is necessary because no empirical equation for this case is known.

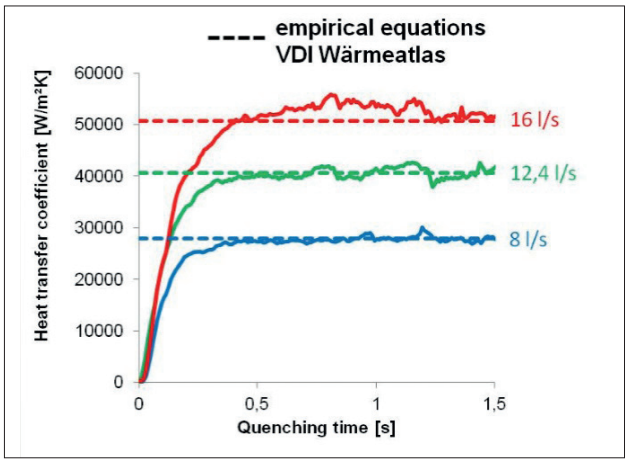

Fig. 3 - Time dependency of heat transfer coefficient (gap flow) for different mass flows in comparison with data from literature [8]

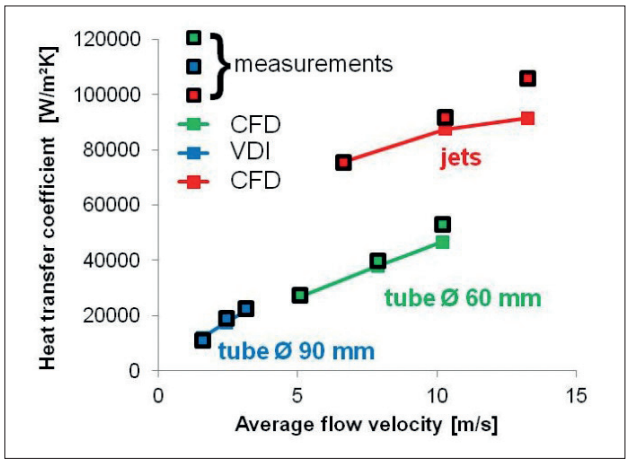

Fig. 4 - Averaged heat transfer coefficients for gap and jet flow in comparison with CFD simulations respectively empirical equations [7]

With these HTC data the Biot numbers of the quenching processes can be calculated according to equation (1).
By use of a value of 22.8 W/(m²K) for the average heat conductivity and the possible ranges of HTC and shaft radius, Biot numbers up to 42 can be produced with the equipment at IWT Bremen.

EXPERIMENTAL RESULTS

Hardness distribution

Maximal and core hardness of all quenched shafts are given in Fig. 5 as function of Biot number. As expected because of the carbon content the maximal hardness of SAE 1055 is higher than for SAE 1035. A similar result was found for the core hardness.

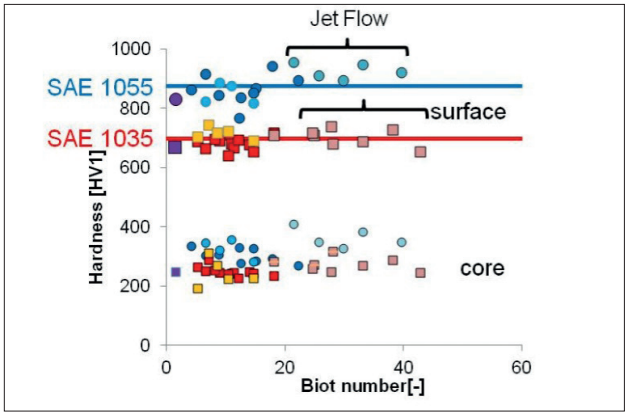

Fig. 5 - Hardness at surface and core of the shafts versus Biot number

The surface hardness scatters around specific mean values for SAE 1035 and SAE 1055. These experimental values are higher than theoretically expected. With the hardness calculation model of Blondeau et al. [9, 10] the theoretical maximal hardness should be approximately 600 HV for SAE 1035 and 750 HV for SAE 1055. The measured mean values were about 100 HV higher than the calculated hardness. The deviation cannot be explained by retained austenite, because the difference is too high. Kobasko [1] explains the higher hardness by a super-strengthening effect due to a higher dislocation density.

Nevertheless it can be stated that all experiments led to a sufficient surface hardness. Therefore the investigated Biot numbers were higher than the lowest Biot number, which is necessary for reaching a sufficient hardness. The values did not fall below this lowest Biot number, neither for SAE 1035 nor for SAE 1055. Furthermore all experiments led to a reduced hardness in the core of the shafts. Hence all experiments resulted in a classical shell hardening. Therefore a critical lowest radius, which is necessary for avoiding through hardening, was not reached for both steel grades, too.

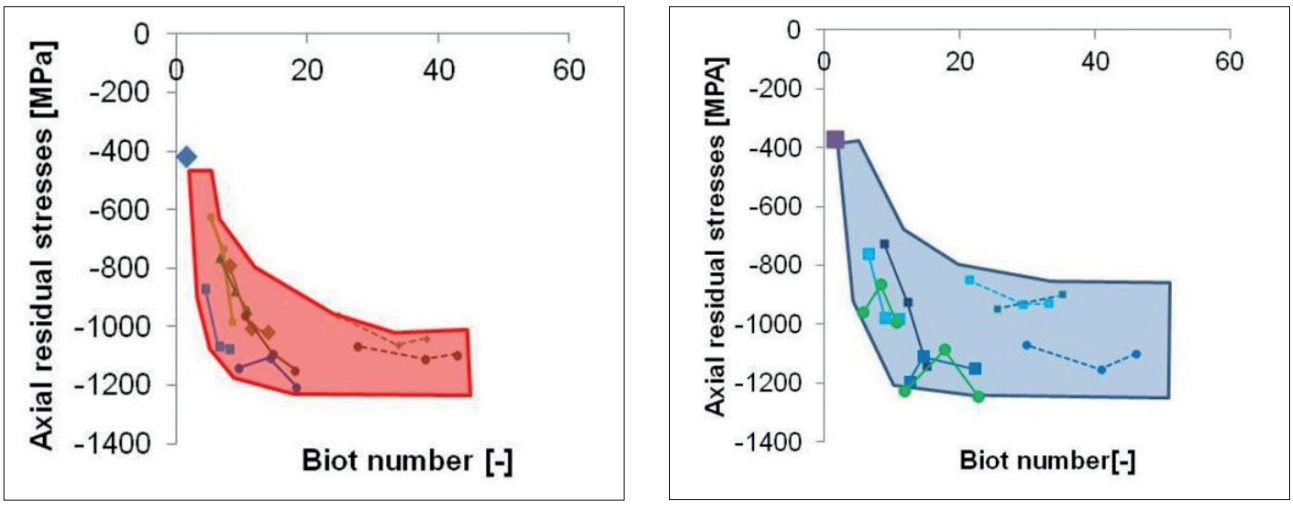

Fig. 6 - Measured residual stresses in axial direction at the surface of the shafts versus Biot number
left: SAE 1035 right: SAE 1055

Residual stresses at the surface

Fig. 6 summarizes the residual stress measurements, which were done by X-ray technology. All quenched cylinders offer compressive residual stresses in the near surface region. Obviously the magnitude of the residual stresses rise with increasing Biot number. The maximum of the compressive residual stresses is about 1200 MPa. For Biot numbers larger than 20, received in the jet quenching tool, no enlargement of the compressive residual stresses was observed.
A critical Biot number for achieving compressive residual stresses at the surface was not found for both steel grades.

PROCESS WINDOWS FOR SHELL HARDENING OF SHAFTS WITH COMPRESSIVE RESIDUAL STRESSES AT THE SURFACE

The experiments have shown that shell hardening of shafts with compressive residual stresses at the surface is much easier to achieve than in the through hardening case. Nevertheless this process will have limits, which were not detected by the experiments. To find these border lines of the process windows, heat treatment simulation was used. Before doing this, a lot of work was necessary to measure the material data and to validate the implemented simulation models. This was done and published in [5]. In this work only one figure from the validation shall be presented that shows the really good agreement between the model and residual stress measurements by thermal neutrons at ILL in Grenoble (Fig. 7) [11].

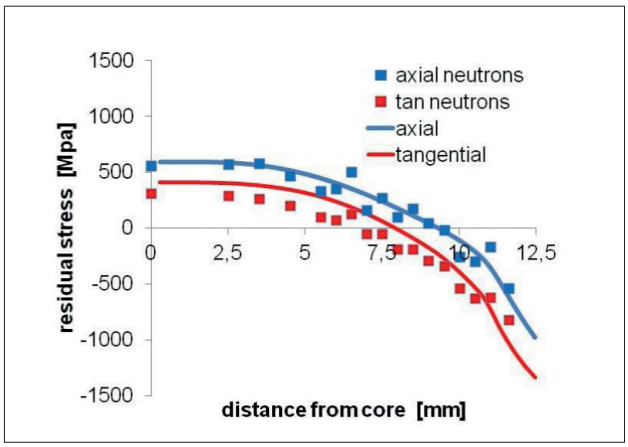

Fig. 7 - Comparison of simulated residual stresses with measurements by thermal neutrons at ILL, Grenoble (Shaft, SAE 1035, Ø 25 mm, HTC about 20 kW/(m²K), SYSWELD)

Definition of shell hardening

To find the process windows at first a quantitative definition of shell hardening is necessary. Here, two conditions must be fulfilled:

- Sufficient hardness at the surface H_{suf}.
- Sufficient hardness difference ΔH between surface and core

But what is a sufficient surface hardness? With respect to heat treatment simulation the following definition was used:

A sufficient surface hardness is given, when the martensite content at the surface is not lower than one percent of the maximum possible value.

The maximum possible martensite amounts depend on the content of retained austenite:

- SAE 1035: M_{max} = 95,5 %
- SAE 1055: M_{max} =91,3 %

By use of the Blondeau model [9, 10] the Vickers hardness of martensite can be estimated by the chemical composition (cf. Table 1) and the cooling rate at 700°C. From this model the sufficient hardness values according to the given definition are:

- SAE 1035: H_{suf} = 570 HV
- SAE 1055: H_{suf} = 750 HV

if the Biot number is less than 20. For the second condition "Sufficient hardness difference ΔH" the following pragmatic definition was used:

A shell hardening is given when the hardness difference between surface and inner regions of the shaft is larger than 50 HV

Determination of the limit for sufficient surface hardness

For each radius of a shaft one critical HTC exists which must be exceeded to avoid more than one percent of diffusive formed phases. By a simulation study with systematic variations of HTC for given radii these critical values were determined.

Determination of the limits for through hardening

For each HTC one critical radius exists which must be exceeded to avoid a hardness difference smaller than 50 HV. By a simulation study with systematic variations of radius for a given HTC these critical values were determined.

Process windows of shell hardening

Fig. 8 visualizes the regions of experimental investigations (colored areas) and summarizes the critical values for HTC and radius. All conditions with larger radius and HTC than the critical values will result in a shell hardened shaft.

As expected the critical data for shell hardening depend on steel grade: The higher hardenability of SAE 1055 results in smaller values for the critical HTC and in larger critical radii than for SAE 1035.

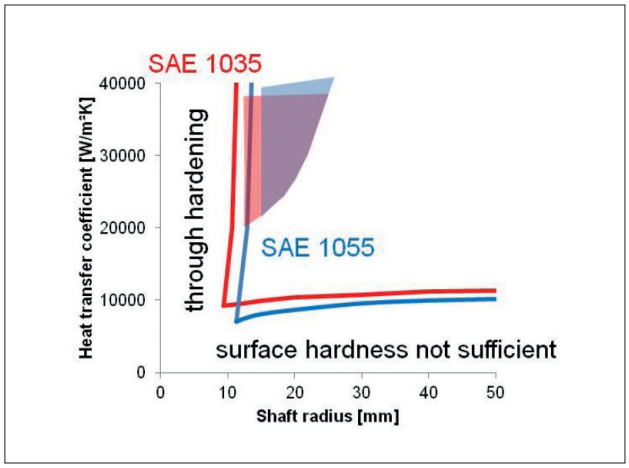

Fig. 8 - Process windows for the investigated melts of SAE 1035 and SAE 1055

Process windows of shell hardening with compressive residual stresses

Finally it has to be checked if inside the complete process windows for shell hardening compressive residual stresses occur. This can be done by simulating the process that belongs to the coordinates of the intersection point of the process windows (lower left corner). Fig. 9 illustrates at first the coordinates of this point for the two investigated steel grades. In Fig. 10 the corresponding residual stresses at the surface are shown: SAE 1035 leads to compressive residual stresses, SAE 1055 to tensile stresses. This means that inside the complete process window for shell hardening compressive residual stresses will be

generated when a critical carbon content will not be exceeded. To determine this value, additional steel grades were modeled by an interpolation respectively extrapolation of the material data of the two investigated steel grades [5]. Fig. 9 shows the resulting carbon dependence of the process window corner and Fig. 10 the corresponding residual stress at the corner points. It can be seen that carbon contents larger than 0.47% will lead to a reduction of the process window for shell hardening with compressive residual stresses.

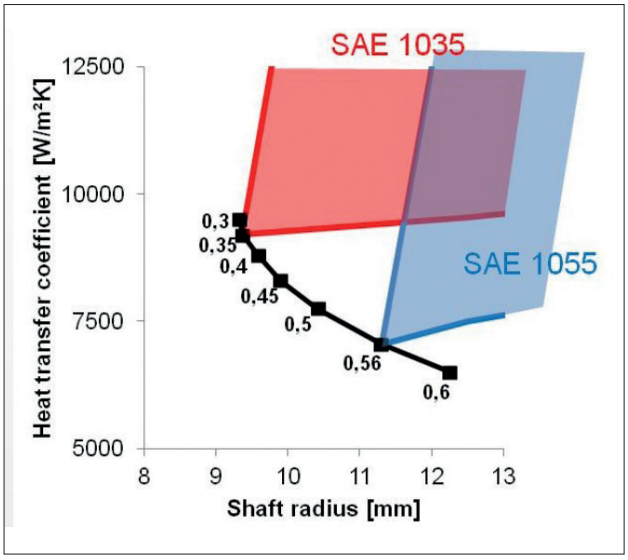

Fig. 9 - Coordinates of process window for shell hardening corner as function of carbon content

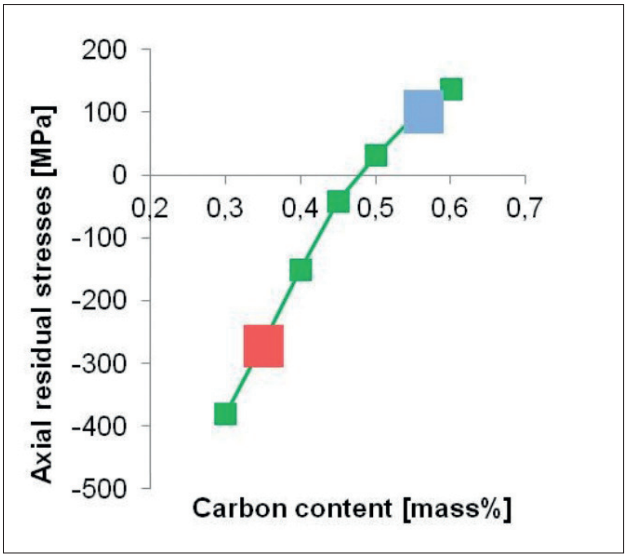

Fig. 10 - Residual stresses in axial direction of process window corner versus carbon content

Fig. 11 shows the reduced process window for SAE 1055. For the generation of compressive residual stresses the possible shaft radii as well as HTC must be further reduced.

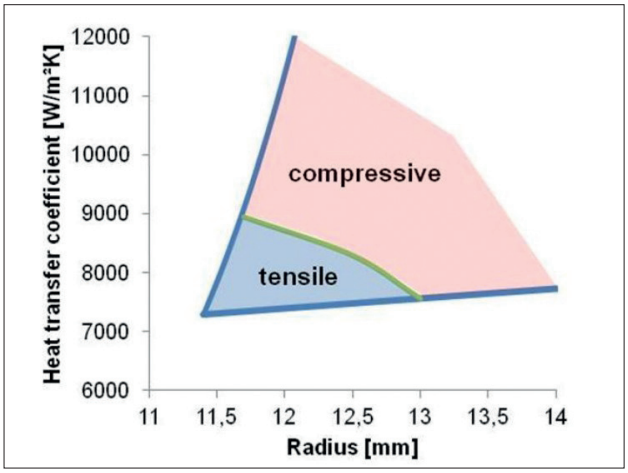

Fig. 11 - Residual stress state of the surface of SAE 1055 shafts in the lower left region of the process window for shell hardening

CONCLUSIONS

The investigations have shown that:

- the IWT equipment enables heat transfer coefficients in the range from 10 - 100 kW/(m²K)
- the compressive stresses rise with increasing Biot number
- Biot numbers higher than 20 seems not to be necessary for shell hardening with compressive residual stresses at the surface
- for shell hardening steel grade dependent process windows exist.
- for shell hardening sufficient work piece dimensions and a heat transfer coefficient larger than about 10 kW/(m²K) are necessary
- for a carbon content less than 0.47 % compressive residual stresses result if shell hardening is achieved
- for higher carbon contents the process windows for compressive residual stresses must be clipped

The reasons for the clipping of the process windows are not fully understood in the moment. One point seems to be the increasing amount of retained austenite with increasing carbon content. Another factor is the difference in the density changes from austenite to the involved ferritic phases and its carbon dependency. To answer these questions further investigations are necessary.

ACKNOWLEDGEMENT

This work was funded by the Federal Ministry for Economic Affairs and Energy. The authors acknowledge the members of the technical committees "Quenching" and "Dimensional and shape changes after heat treatment" for their support of the project. Furthermore the authors wish to acknowledge Thilo Pirling, ILL, Grenoble, and Jeremy Epp, IWT Bremen, for the measurements and evaluation with thermal neutrons at ILL in Grenoble and Udo

Fritsching, Sören Sander, and Sven Schüttenberg, IWT Bremen for the calculation of HTC and the optimization of the flow field in the quenching tools by CFD simulation.

REFERENCES

[1] Kobasko, N.I. Aronov, M.A. Powell, J.A and Totten, G.E., Intensive Quenching Systems, Engineering and Design. ASTM International, West Conshohocken PA (2010).

[2] Rath, J.; Lübben, Th.; Hunkel, M.; Hoffmann, F.; Zoch, H.-W.: Basic researches about the generation of compressive residual stresses by High Speed Quenching. HTM J. Heat Treatm. Mat. 64 (2009) 6, S. 338 - 350 (in German).

[3] Rath, J.; Lübben, Th.; Hoffmann, F.; Zoch, H.-W.: Generation of Compressive Residual Stresses by High-Speed Water Quenching. Proc.4th Int. Conf. Thermal Process Modeling and Computer Simulation (on CD), Shanghai, China (2010).

[4] D.P. Koistinen, R.E. Marburger, Acta Metall. 7 (1959) 59-60.

[5] Frerichs, F.; Lübben, Th.: Simulation of shell hardening of unalloyed steel cylinders due to high speed quenching. Proc. 5th Int. Conf. Thermal Process Modeling and Computer Simulation, Orlando, Florida, US (2014), p. 260-268.

[6] Frerichs, F.; Lübben, Th.; Hoffmann, F.; Zoch, H.-W.: Shell hardening of unalloyed steel cylinders due to high speed quenching. Proc. European Conf. Heat Treatment and 21st IFHTSE Congr., Munich, Germany (2014), p. 275-282.

[7] Frerichs, F.; Sander, S.; Lübben, Th.; Schüttenberg, S.; Fritsching, U.: Determination of Heat Transfer Coefficients in High Speed Quenching Processes. Materials Performance and Characterization, Vol 3, No. 4, 2014, doi: 10.1520/MPC20130112.

[8] Verein Deutscher Ingenieure (VDI-GVC) (Hrsg.), "VDI WÄRMEATLAS. Recherchieren - Berechnen - Konstruieren", 11th ed., Springer Verlag, Berlin, 2013.

[9] Blondeau, R. Maynier Ph., Dollet J, .Mem Sci. Rec. Metallurgie, Vol. 70, No. 12 (1973), pp. 883-892.

[10] Blondeau, R. Maynier Ph., Dollet J., Vieillard-Baron B., Mem Sci. Rec. Metallurgie, Vol. 72 (1975), pp. 759-769.

[11] Frerichs, F.; Fritsching, U.; Lübben, Th.; Sander, S.; Schüttenberg, S.: Schalenhärtung mittels Hochgeschwindigkeits-Abschreckung - Teil 2. HTM J. Heat Treatm. Mat. 70, (2015) 3, S. 123-134.